Estimating land surface albedo from polar orbiting and geostationary satellites

Dongdong Wang
Shunlin Liang
Tao He
Yuan Zhou
Department of Geographical Sciences
University of Maryland, College Park
Nov 13 2014

$$R_n = R_n^s + R_n^l = (1-\alpha)F_d^s + F_d^l - \sigma\varepsilon T^4$$

Net radiation

albedo

Insolation

Emissivity

Longwave downward radiation

Skin temperature

Radiation budget

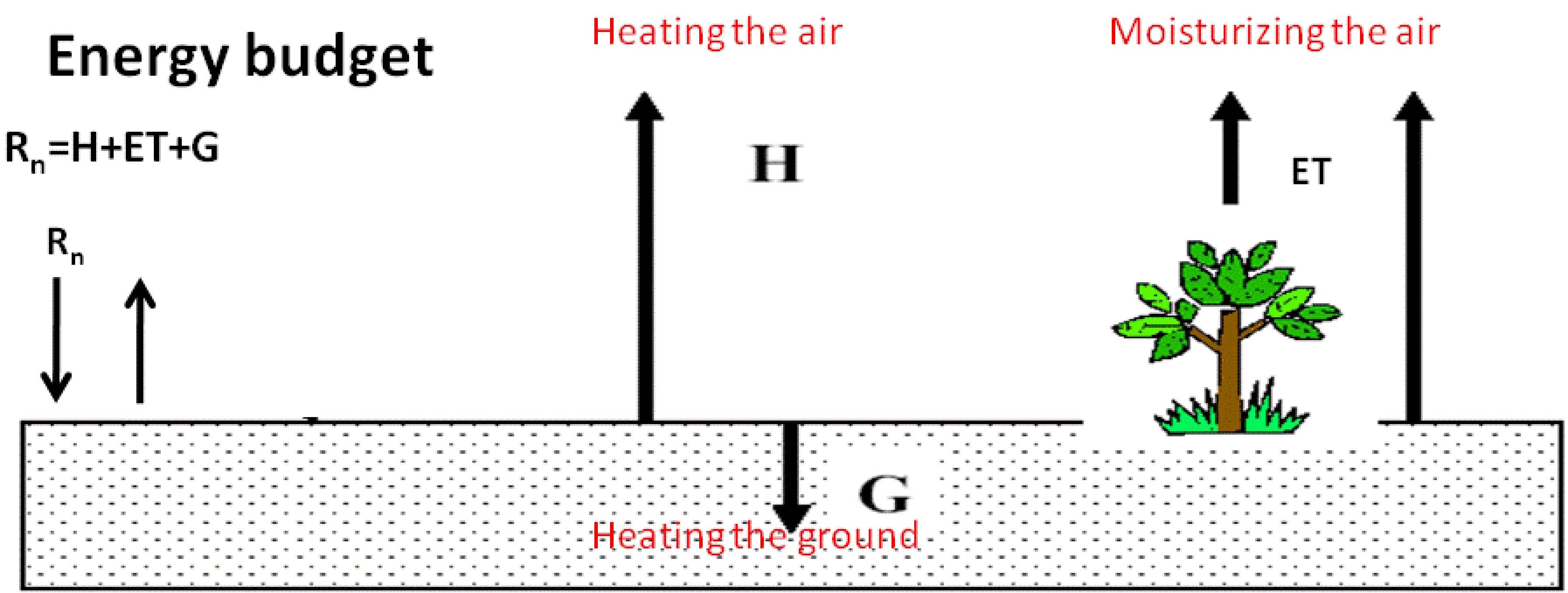

Land surface albedo (LSA) in the climate system

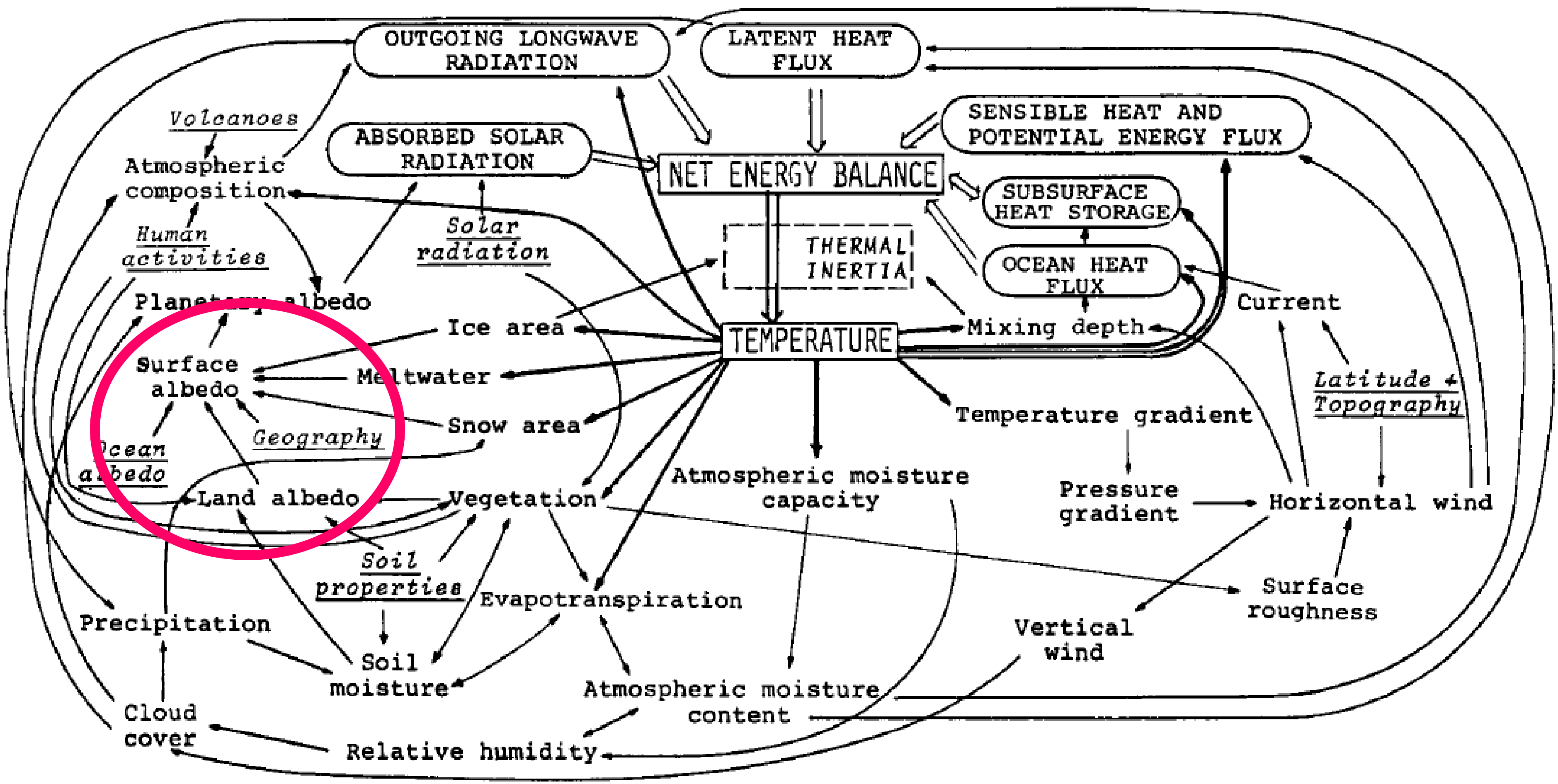

FIG. 1. Climate feedback diagram.

(Robock, 1985)

LSA vs weather and climate modeling

- Accurate representation of surface characteristics is important for weather prediction and climate modeling.
- Use of real-time satellite LSA products can improve forecasts of surface temperature, specific humidity, and wind speed etc.

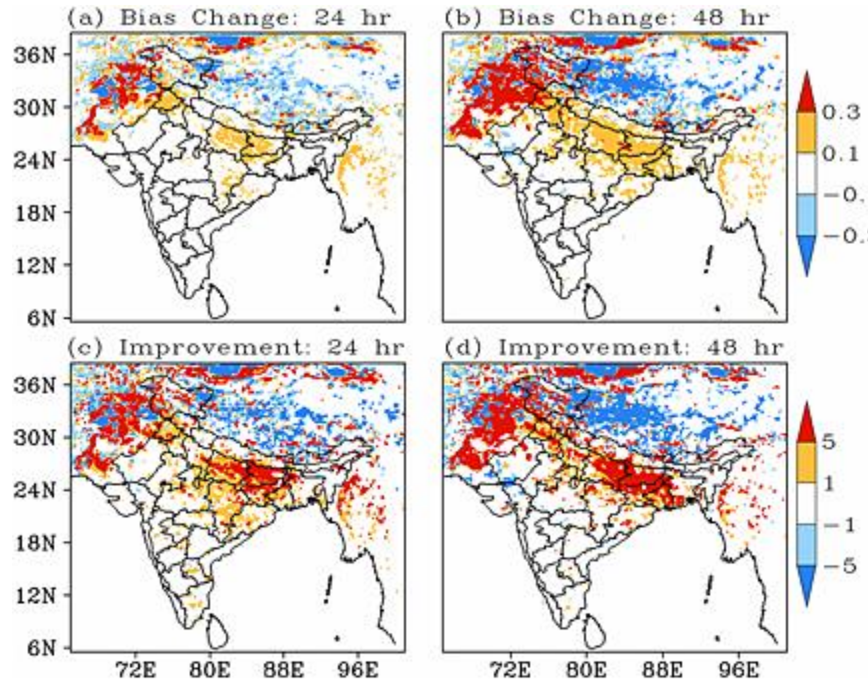

Spatial distribution of BIAS change (°C) in (a) 24 h and (b) 48 h 2 m temperature forecast and improvement parameter (%) in (c) 24 h and (d) 48 h 2 m temperature forecast from KAL experiment compared to control experiment where the changes are statistically significant at 90% confidence level. (Kumar et al. 2014, JGR)

Uncertainties in current LSA datasets

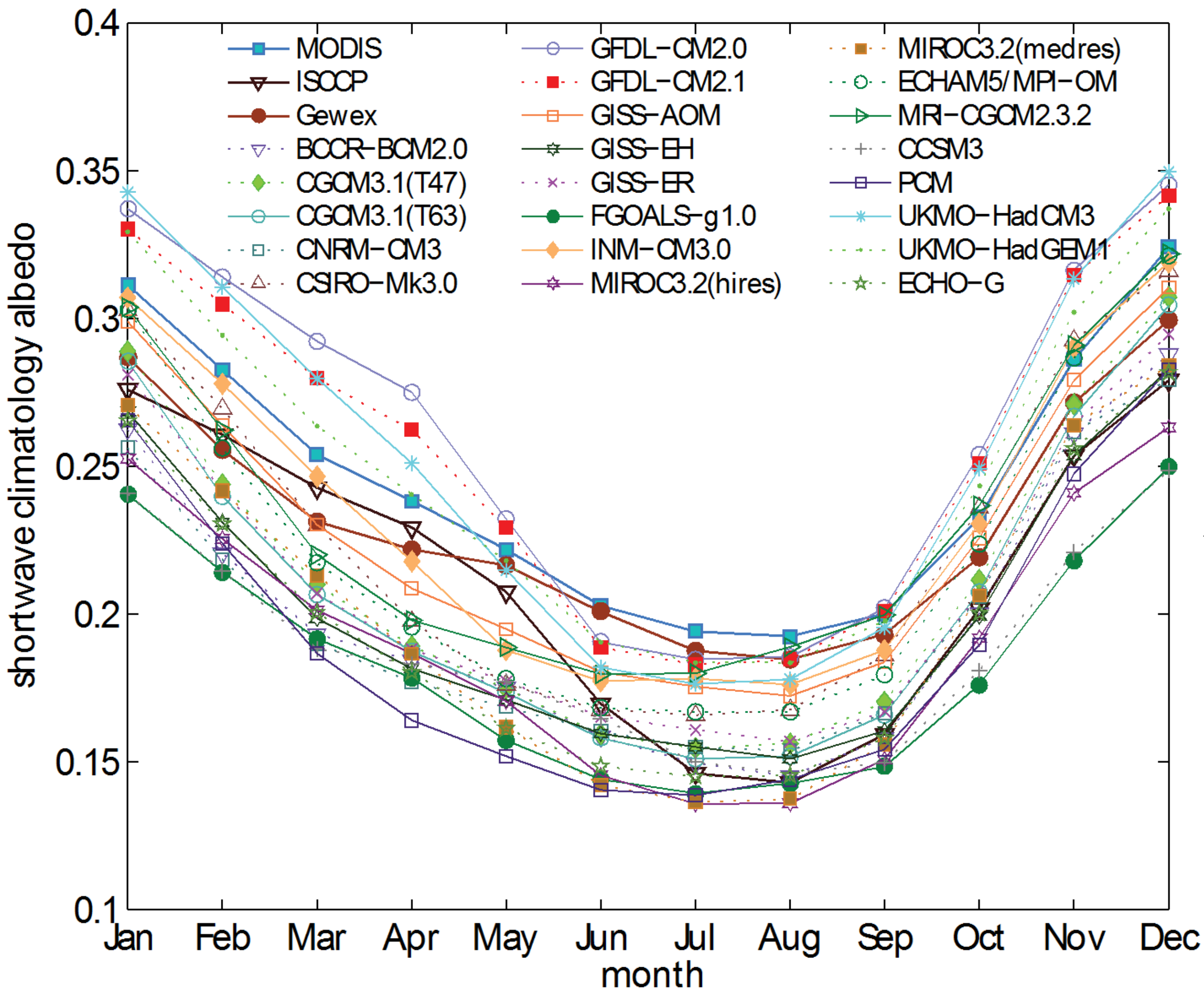

Zhang, X. **S. Liang**, K. Wang, L. Li, and S. Gui, (2010), A climatological analysis of global land surface shortwave broadband albedo from MODIS, *IEEE Journal of Special Topics in Applied Earth Observations and Remote Sensing*, 3:296-305

Model mean: 0.21
Standard dev.: 0.02

MODIS: 0.24

IPCC AR4 GCM model simulations and satellite products

Remote sensing of LSA: MODIS algorithm

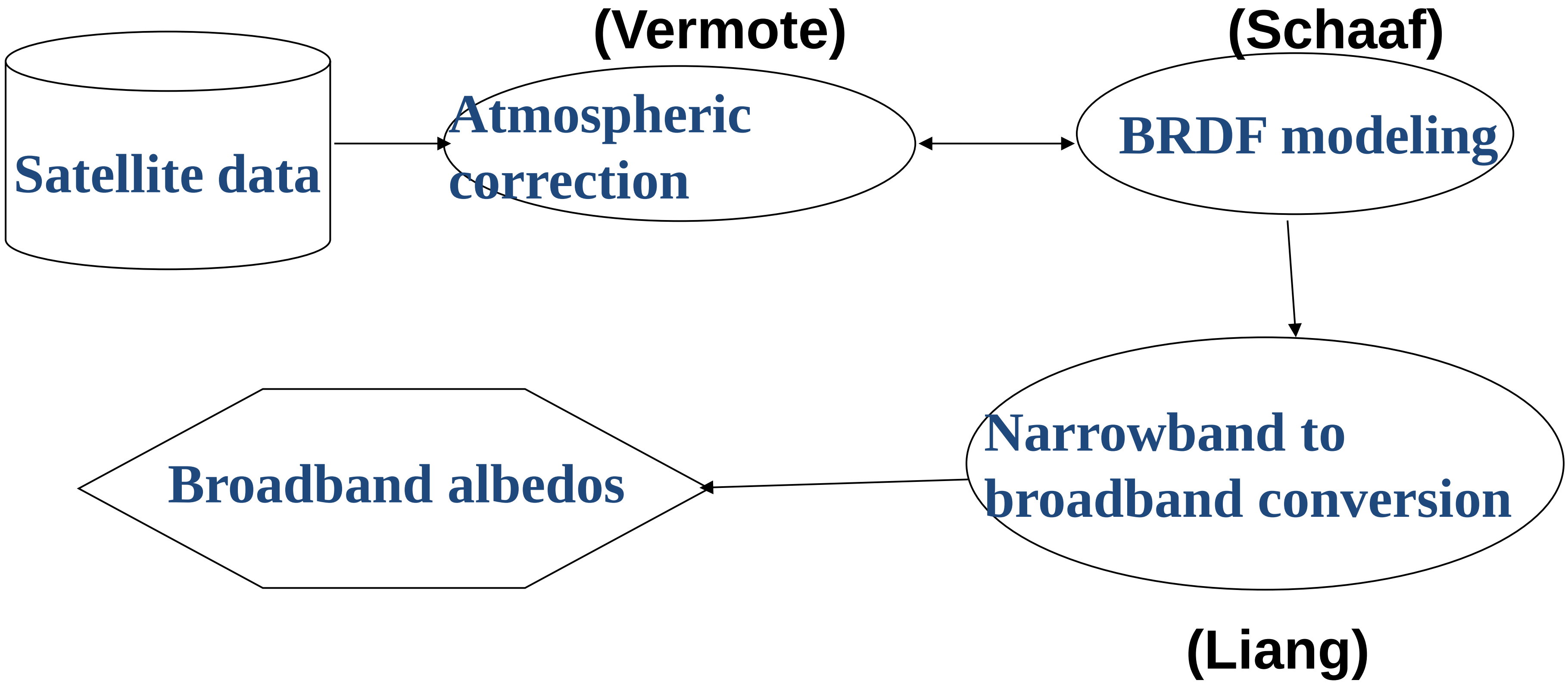

- Traditional algorithms to estimate LSA from satellite top-of-atmosphere (TOA) signature
- Multiple temporal information is used to model surface anisotropy of reflectance.

Remote sensing of LSA: direct estimation

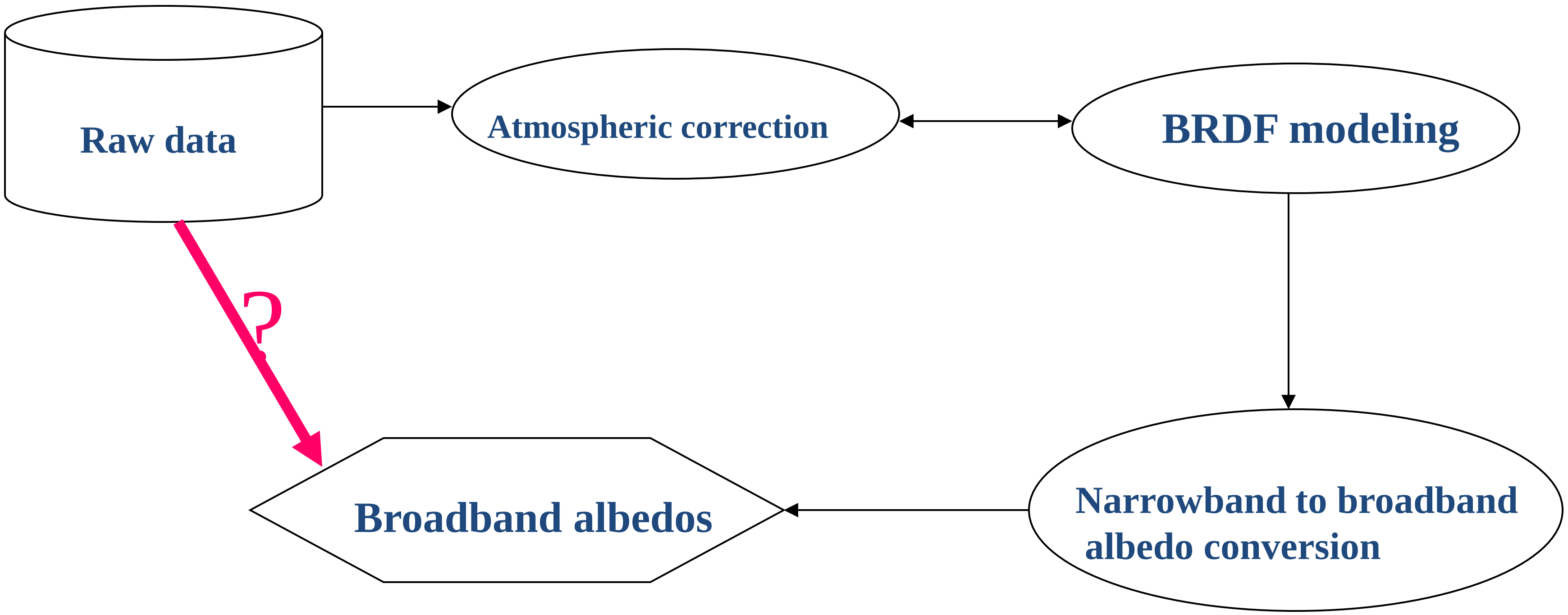

Liang, S., A direct algorithm for estimating land surface broadband albedos from MODIS imagery, *IEEE Trans. Geosci. Remote Sen.*, 41(1):136-145, 2003*;*

Liang, S., J. Stroeve and J. Box, (2005), *Mapping daily snow shortwave broadband albedo from MODIS: The improved direct estimation algorithm and validation, Journal of Geophysical Research. 110 (D10): Art. No. D10109.*

VIIRS surface albedo EDR

- Visible Infrared Imaging Radiometer Suite (VIIRS) is a multispectral sensor onboard the Suomi National Polar-orbiting Partnership (NPP) and future Joint Polar Satellite System (JPSS) satellites.
- Surface albedo is produced from VIIRS as Environmental Data Record (EDR).
- Surface albedo EDR is combination of land surface albedo (LSA), ocean surface albedo (OSA) and sea-ice surface albedo (SSA).
- Bright Pixel Sub-Algorithm (BPSA) is currently used to generate LSA from VIIRS data. Several improvements have been made since the S-NPP launch.

VIIRS spectral characteristics

Band No.	Center Wavelength (μm)	Equiv. Width (μm)
M1	0.411	0.0198
M2	0.444	0.0143
M3	0.486	0.0190
M4	0.551	0.0209
I1	0.639	0.0775
M5	0.672	0.02
M6	0.745	0.0146
I2	0.862	0.0394
M7	0.862	0.0387
M8	1.238	0.0271
M9	1.375	0.0150
I3	1.602	0.0572
M10	1.602	0.0587
M11	2.257	0.0467
I4	3.753	0.360
M12	3.697	0.192
M13	4.067	0.165
M14	8.578	0.324
M15	10.729	0.990
I5	11.469	1.75
M16	11.845	0.866

Cao et al., 2013, JGR

Example of VIIRS LSA: temporal composite

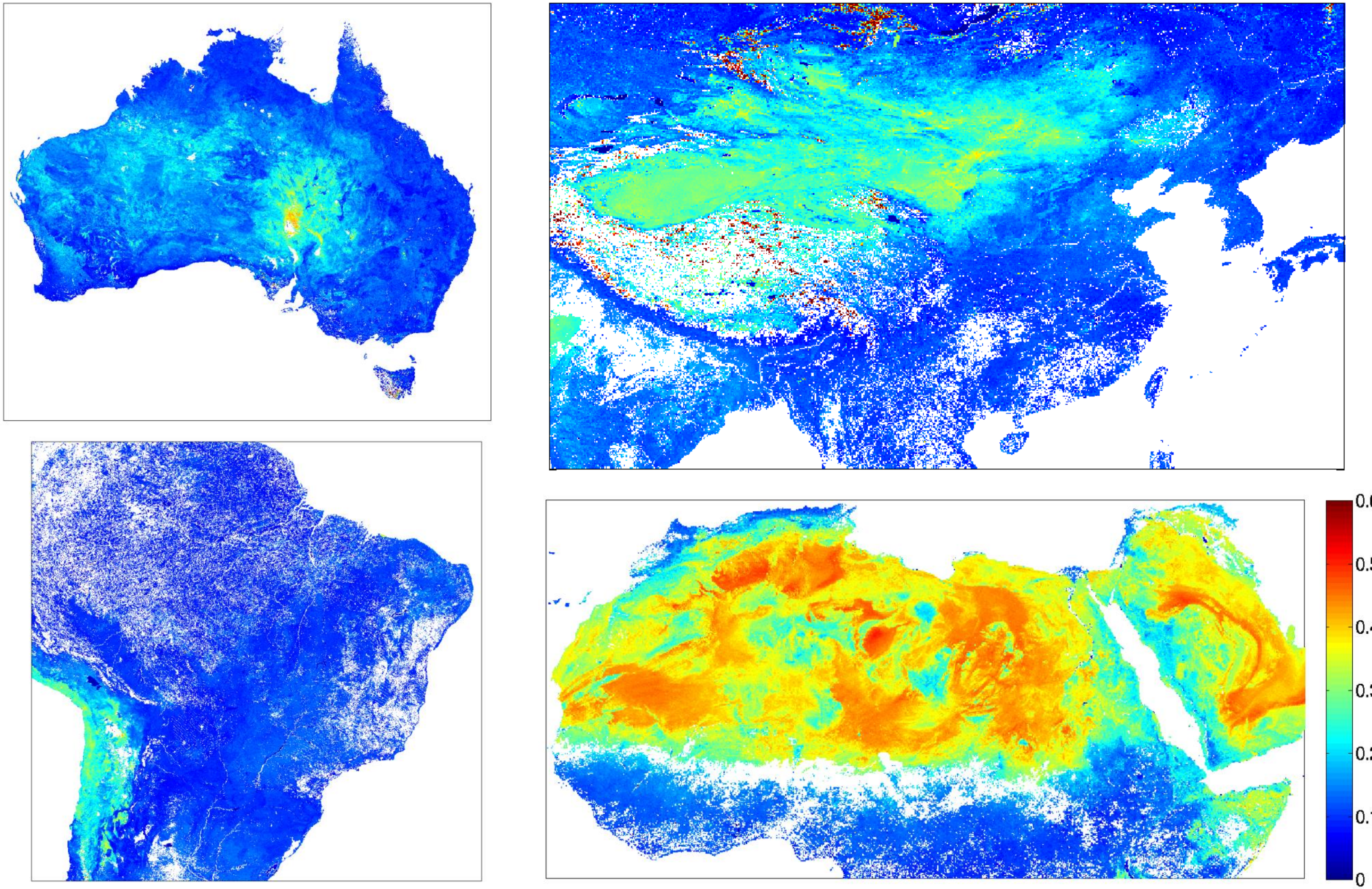

Temporal averaged maps of surface albedo, May 8-23, 2012

Refinement to the BPSA algorithm

- A new LUT of LSA BPSA regression coefficients was developed:
  - Using updated spectral response function;
  - Considering multiple aerosol types;
  - Including surface BRDF in radiative transfer simulation;
  - Developing surface-specific LUTs.

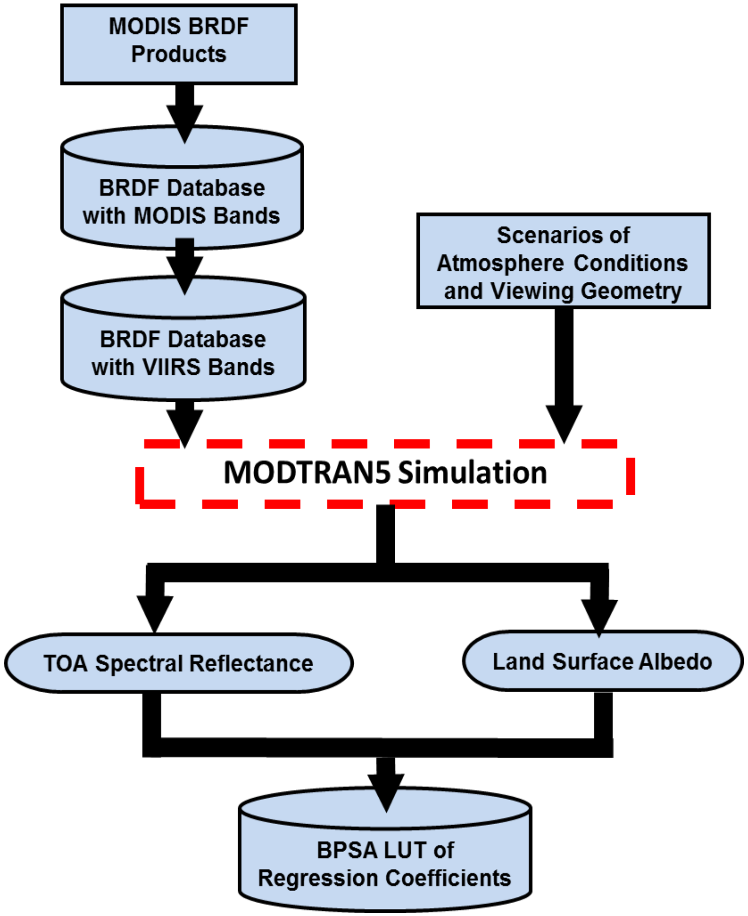

Modeling atmospheric radiative transfer

Incorporation of surface BRDF:

$$T(\theta_s) = \left[\, t_{dd}(\theta_s) \quad t_{dh}(\theta_s) \,\right],$$

$$T(\theta_v) = \left[\, t_{dd}(\theta_v) \quad t_{hd}(\theta_v) \,\right]^T,$$

$$\rho = \rho_0 + \frac{T(\theta_s)R(\theta_s,\theta_v,\phi)T(\theta_v) - t_{dd}(\theta_s)t_{dd}(\theta_v)\left|R(\theta_s,\theta_v,\phi)\right|\bar{\rho}}{1 - r_{hh}\bar{\rho}}$$

$$R(\theta_s,\theta_{v,}\varphi) = \begin{bmatrix} r_{dd}(\theta_s,\theta_{v,}\varphi) & r_{dh}(\theta_s) \\ r_{hd}(\theta_v) & r_{hh} \end{bmatrix}.$$

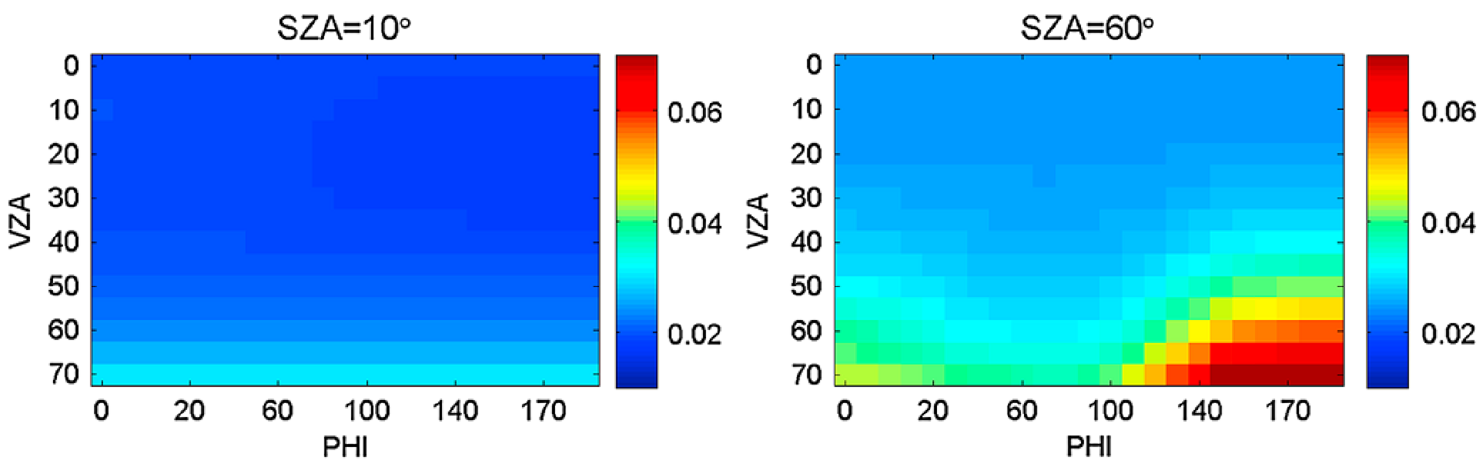

Figure 2. Predictability (in terms of RMSE) of the regression models varies with viewing geometry. Results shown here are from the generic LUT with surface BRDF at two solar zenith angles (10° and 60°).

Wang, D.D., Liang, S.L., He, T., & Yu, Y.Y. (2013). Direct estimation of land surface albedo from VIIRS data: Algorithm improvement and preliminary validation. *Journal of Geophysical Research-Atmospheres, 118*, 12577-12586, doi: 10.1002/2013jd020417.

Validating VIIRS LSA: SURFRAD stations

- Seven NOAA SURFRAD sites
- http://www.esrl.noaa.gov/gmd/grad/surfrad
- Surface Radiation Budget Network, established in 1993
- Bondville is not used due to great spatial heterogeneity
- Instantaneous measurements of downward and upward shortwave radiation at the surface every minute

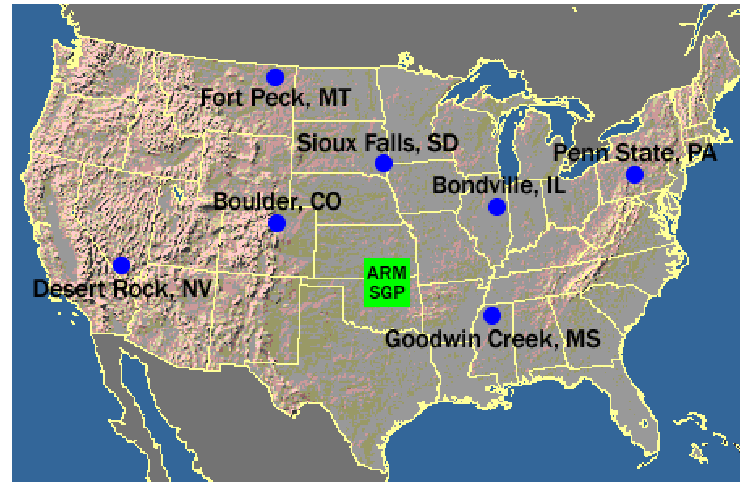

Short name	Location	Latitude	Longitude	Land cover
DRA	Desert Rock, NV	36.63	-116.02	Desert
BON	Bondville, IL	40.05	-88.37	Cropland
FPK	Fort Peck, MT	48.31	-105.10	Grassland
GWN	Goodwin Creek, MS	34.25	-89.87	Forest/Pasture
PSU	Penn State, PA	40.72	-77.93	Cropland
SXF	Sioux Falls, SD	43.73	-96.62	Grassland
TBL	Boulder, CO	40.13	-105.24	Grassland

Bright surface

Dark surface

Validation of 16-day mean VIIRS LSA

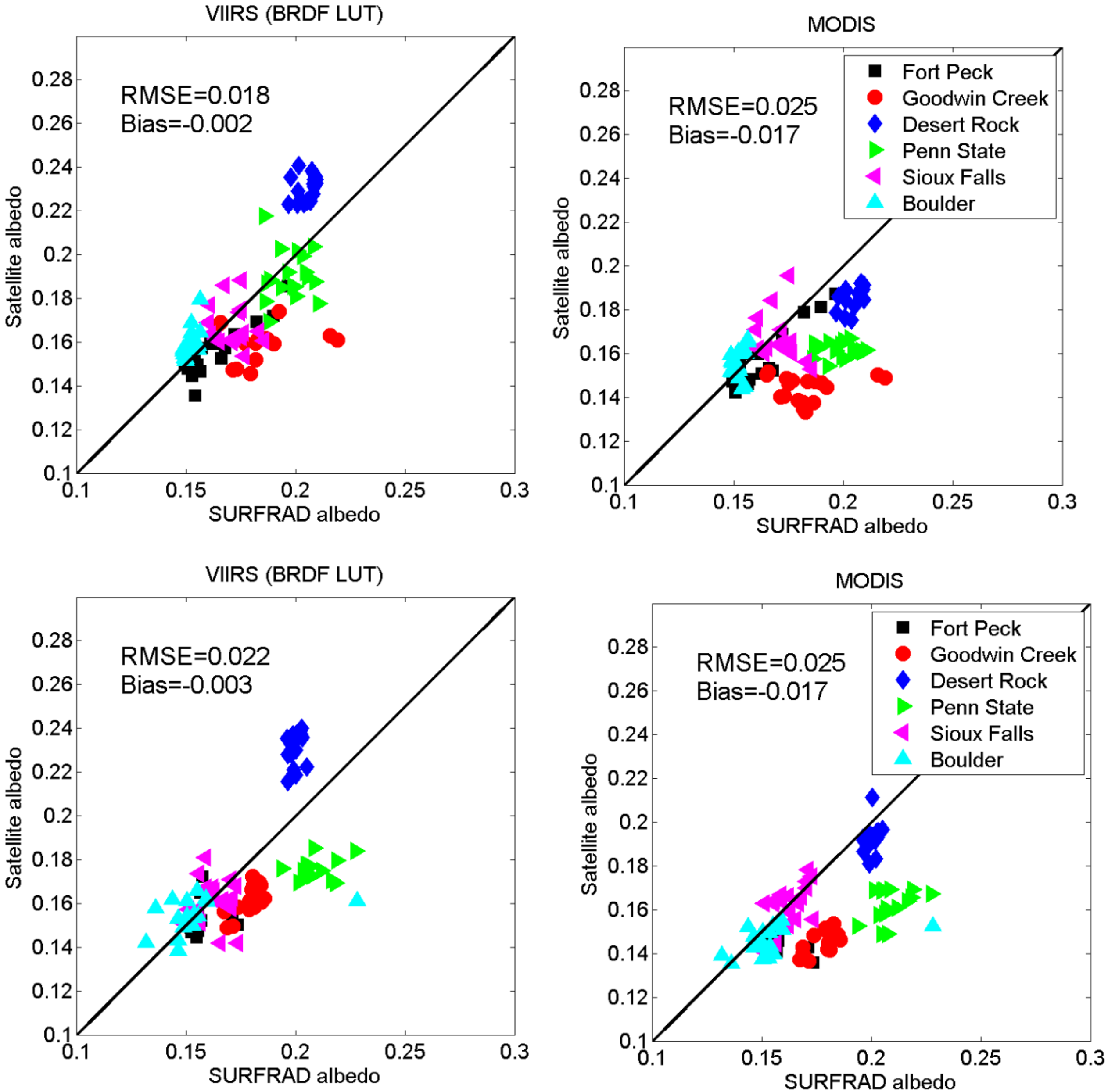

Validation results of 16-day mean albedo from VIIRS BRDF LUT and MODIS, using data from non-snow seasons (May-September) at seven SURFRAD sites for two years: 2012 (top) and 2013 (bottom).

Evaluation of temporal variability of VIIRS LSA

- BPSA LSA is retrieved from one single clear-sky observations. Residual variations may still exist over stable surfaces after incorporation of surface BRDF modeling.
- The LSA retrievals in the summer of 2012 over two Libya desert sites (Site 1: 24.42˚N 13.35˚E and Site 2: 26.45˚N, 14.08˚E) are used to illustrate the issue of temporal variability of LSA.

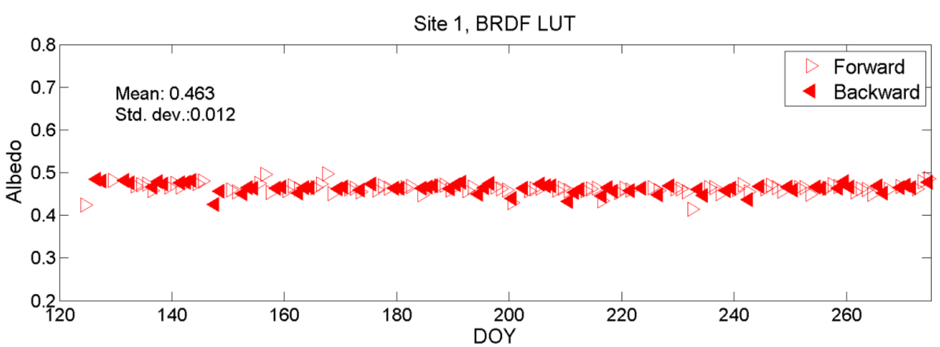

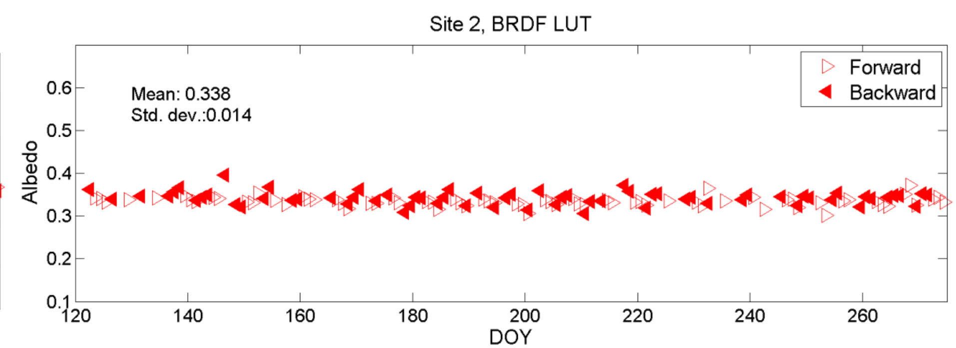

Residue of BRDF fitting, calculated as the difference between MODIS surface reflectance and BRF predicted from MODIS BRDF. The narrow-to-broadband conversion coefficients are used to covert spectral residues to the broadband residue.

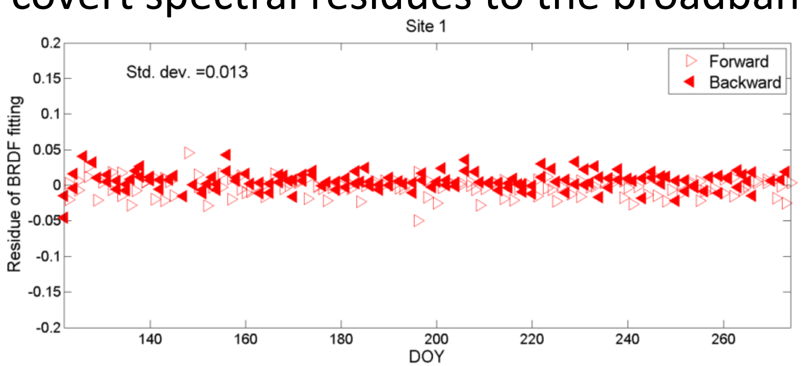

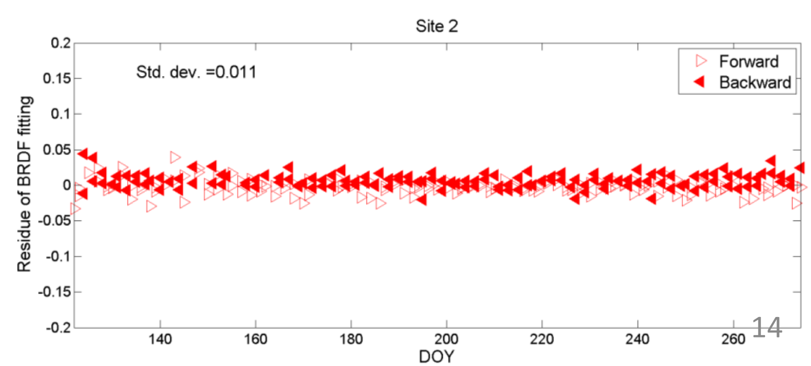

Maps of 16-day mean albedo

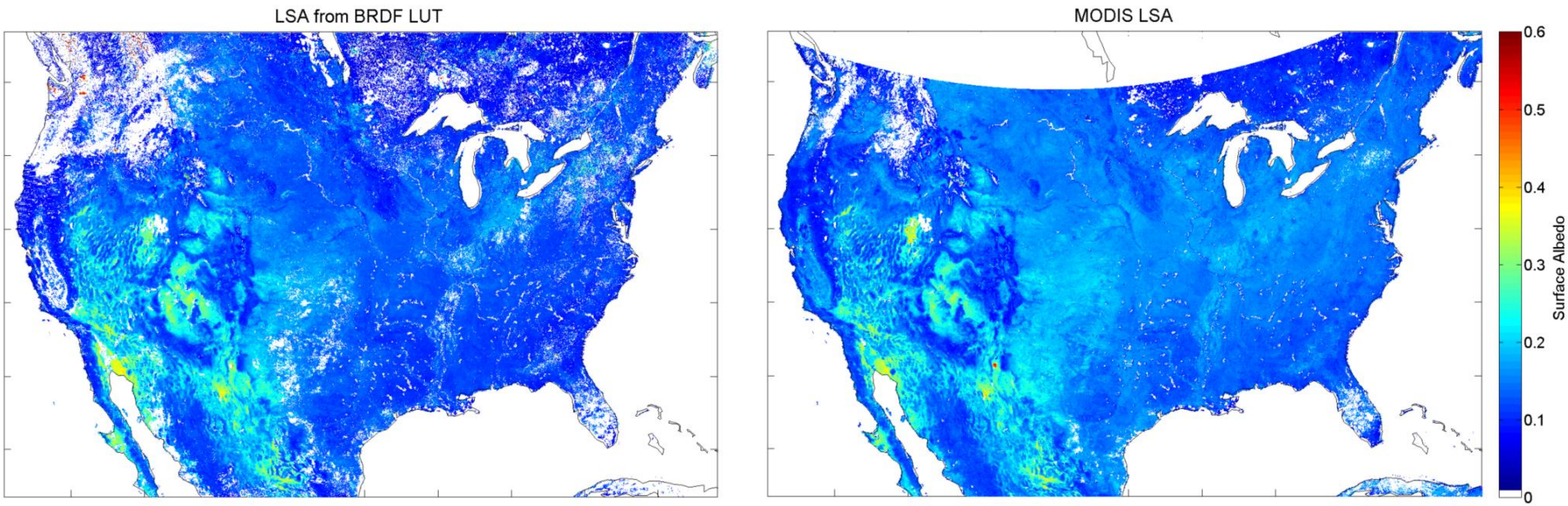

Contiguous US maps of 16-day mean LSA from VIIRS and MODIS, during DOY 145-160, 2012

Comparing 16-day mean VIIRS albedo from BRDF LUT with MODIS blue-sky albedo. Data are limited to those with at least 8 clear-day observations during the composite period of 16 days.

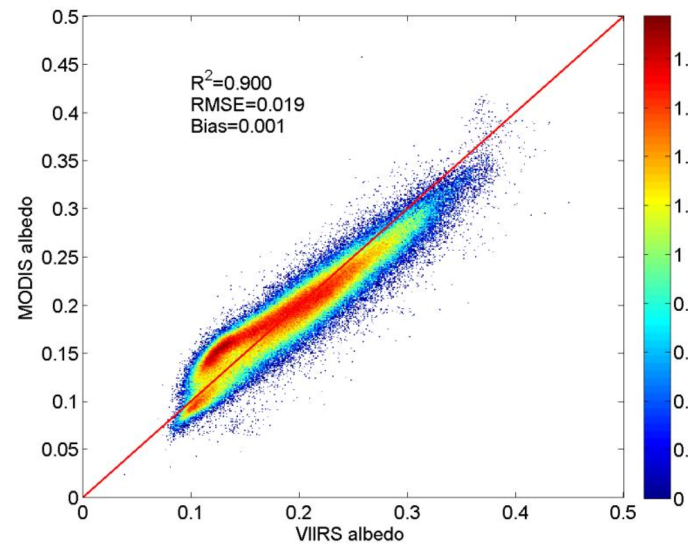

Remote sensing of LSA: optimization

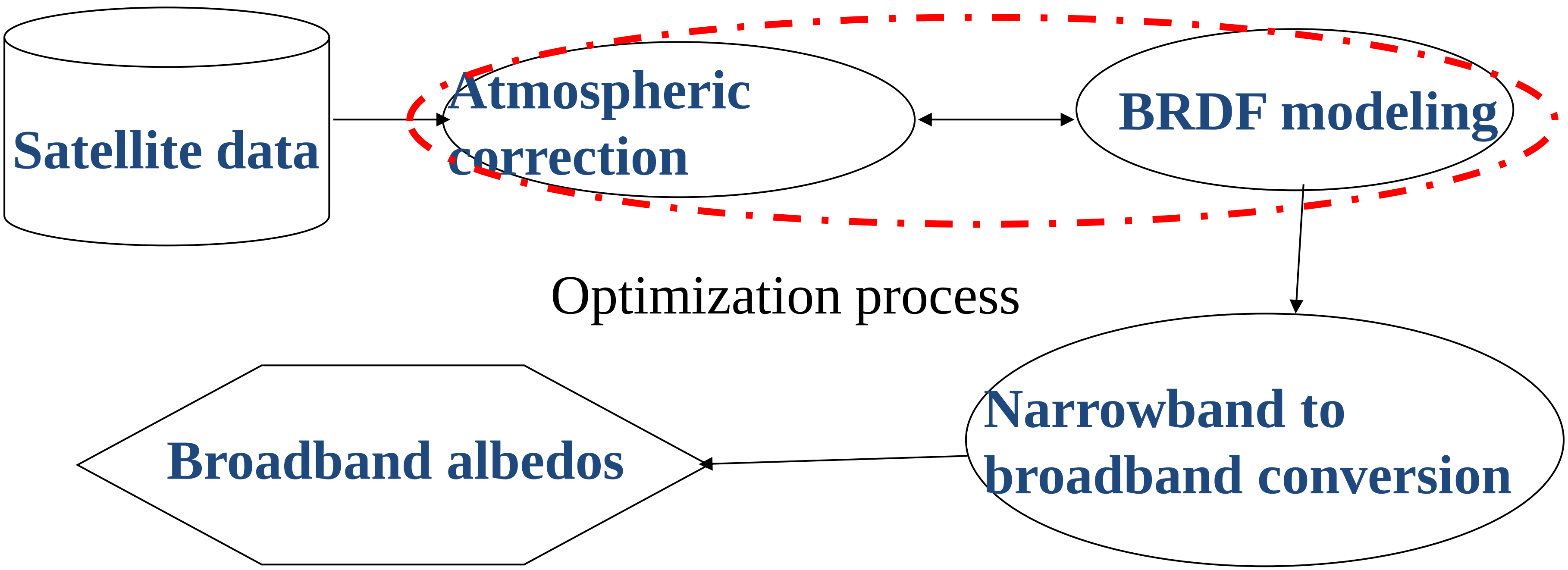

16

Developing algorithms for GOES-R

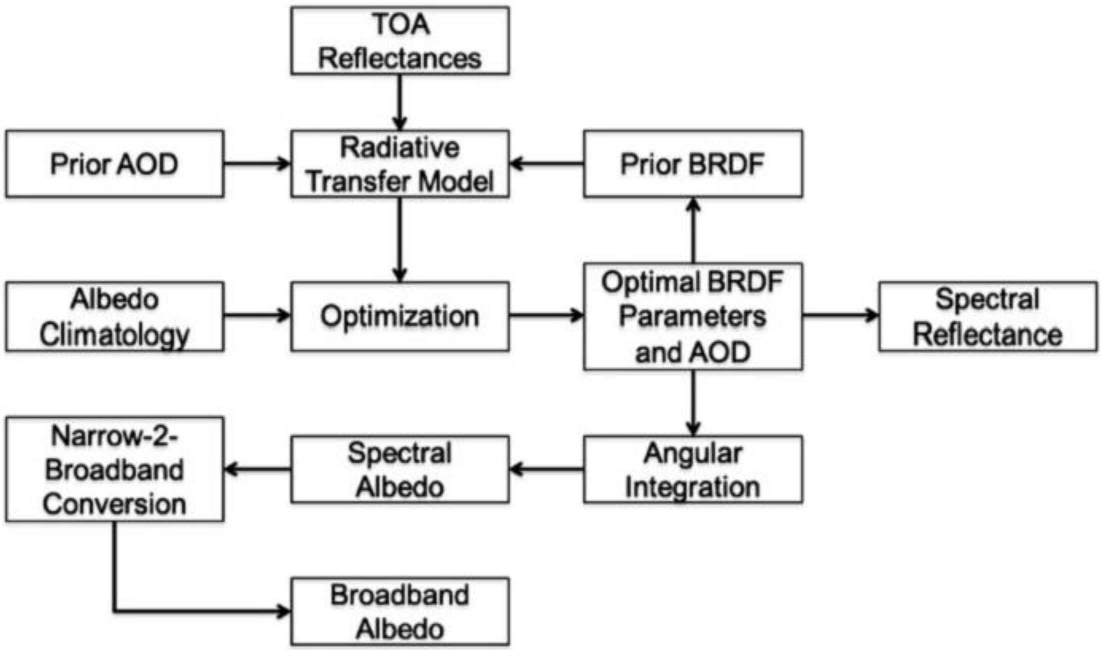

	ABI	Current GOES Imager
Spectral Coverage	16 bands	5 bands
Spatial Resolution		
0.64 µm Visible	0.5 km	~ 1 km
Other visible/near-IR	1.0 km	n/a
Bands (>2 µm)	2 km	~ 4 km
Spatial Coverage		
Full Disk	4 per hour	Scheduled (3 hrly)
CONUS	12 per hour	~4 per hour
Mesoscale	Every 30 sec	n/a
Visible (reflective bands)		
On-orbit calibration	Yes	No

http://www.goes-r.gov/spacesegment/abi.html

He, T., Liang, S., Wang, D., Wu, H., Yu, Y., & Wang, J. (2012). Estimation of surface albedo and directional reflectance from Moderate Resolution Imaging Spectroradiometer (MODIS) observations. *Remote Sensing of Environment, 119*, 286-300, doi: 10.1016/j.rse.2012.01.004.

Prototyping GOES-R algorithm: results

Table 5
Statistics of the retrieved values from this study with comparison to ground measurements over SURFRAD sites.

(a)

Site name	Bias	RMSE	R^2
Bondville	−0.0097	0.0615	0.6268
Boulder	0.0245	0.0781	0.0086
Desert Rock	−0.0033	0.0271	0.0013
Fort Peck	0.0241	0.0541	0.9714
Goodwin Creek	−0.0403	0.0581	0.1035
Penn State	−0.0135	0.0390	0.4537
Sioux Falls	−0.0031	0.0762	0.7884
All sites for no snow	−0.0016	0.0268	0.0783
All sites for snow	0.0324	0.1319	0.3855

(b)

Site name	Retrieved AOD vs ground measurements		MODIS AOD vs ground measurements	
	Bias	RMSE	Bias	RMSE
Bondville	0.0529	0.1283	0.0579	0.1416
Boulder	−0.0059	0.0567	0.0025	0.0612
Desert Rock	0.0186	0.0451	n/a	n/a
Fort Peck	0.0330	0.0654	0.0357	0.0986
Goodwin Creek	0.0095	0.1271	−0.0445	0.1290
Penn State	n/a	n/a	n/a	n/a
Sioux Falls	0.0232	0.0901	−0.0480	0.1210
All sites	0.0243	0.0984	−0.0009	0.1187

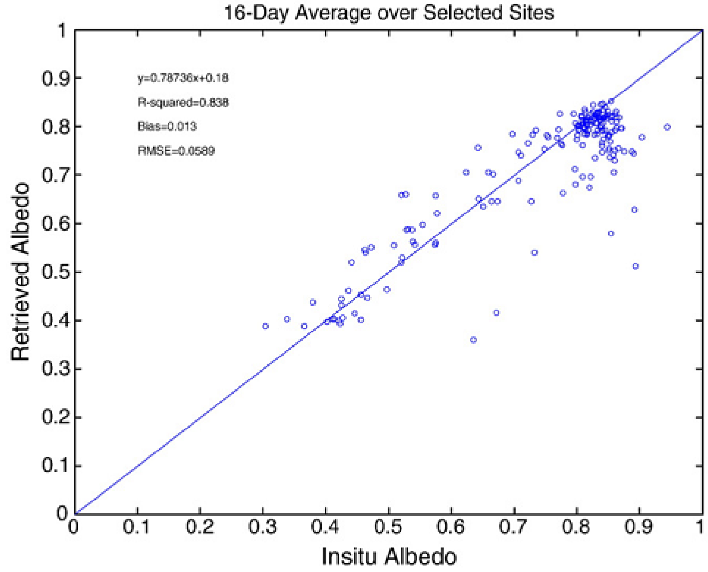

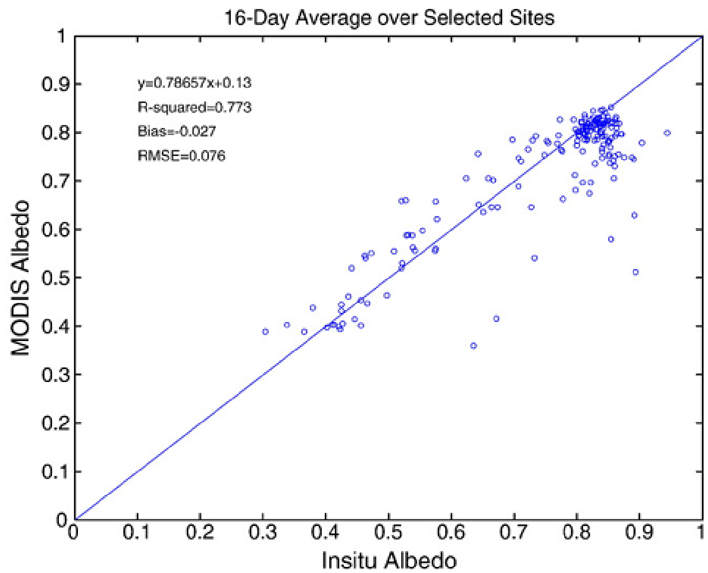

He, T., Liang, S., Wang, D., Wu, H., Yu, Y., & Wang, J. (2012). Estimation of surface albedo and directional reflectance from Moderate Resolution Imaging Spectroradiometer (MODIS) observations. *Remote Sensing of Environment, 119*, 286-300, doi: 10.1016/j.rse.2012.01.004.

Estimating LSA from hyperspectral data: AVIRIS

- Airborne Visible InfraRed Imaging Spectrometer (AVIRIS) is a airborne hyperspectral sensor.
- It has 224 spectral channels with wavelengths from 400 to 2500 nm.
- AVIRIS is used in NASA HyspIRI Preparatory Airborne Campaign.
- We are funded by NASA to estimate quantities surface radiation budget (including land surface albedo) from HyspIRI-like data.

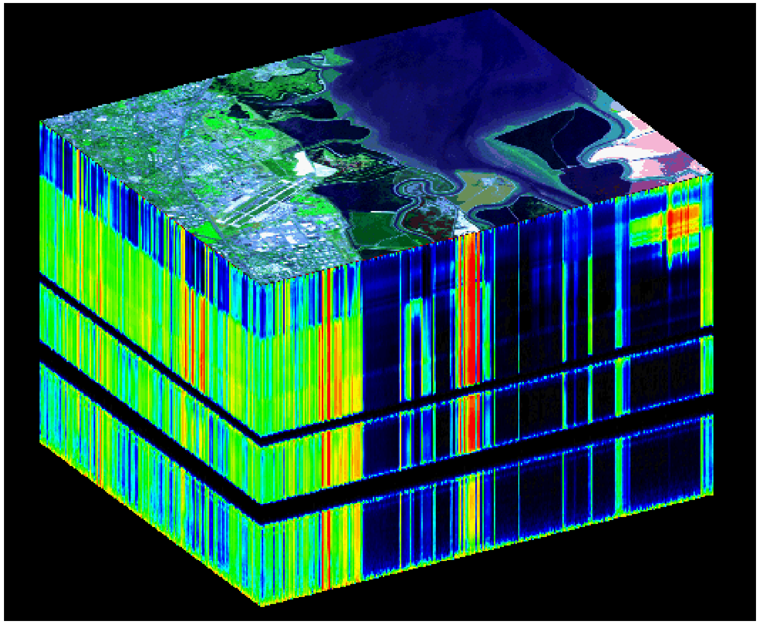

http://aviris.jpl.nasa.gov/data/image_cube.html

Spectral vs. angular information in broadband albedo direct estimation

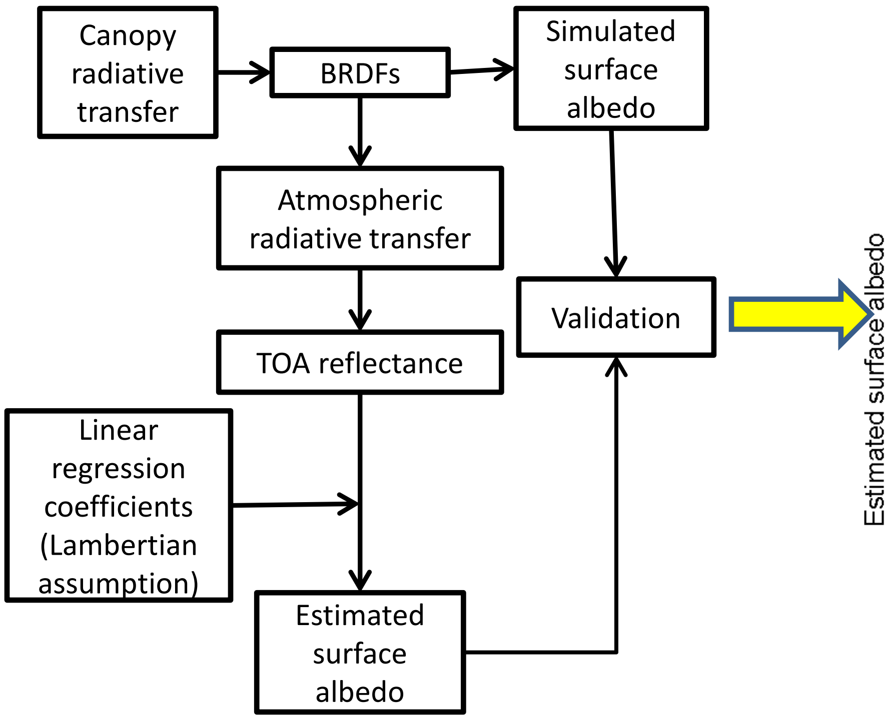

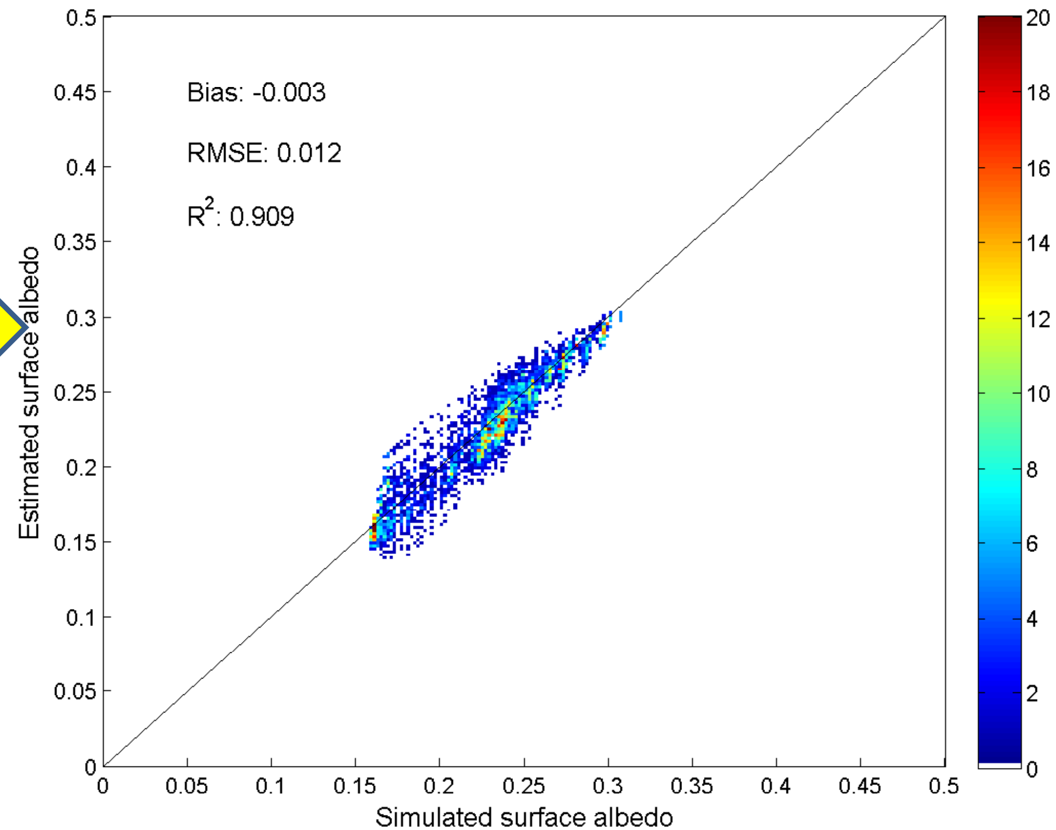

Hyperspectral information is MORE important than angular information in surface broadband albedo estimation for snow-free surfaces

Albedo estimation accuracy and view zenith angle (solar zenith angle=35°)

Variable	Value				
View zenith angle (°)	0	15	30	45	60
RMSE	0.0155	0.0100	0.0091	0.0104	0.0147
R^2	0.9181	0.9505	0.9493	0.9261	0.8596

He, T., S. Liang, D. Wang, and Q. Shi, (2014). Estimation of high-resolution land surface shortwave albedo from AVIRIS data. *IEEE JSTARS, in press*

Validation of AVIRIS albedo estimates

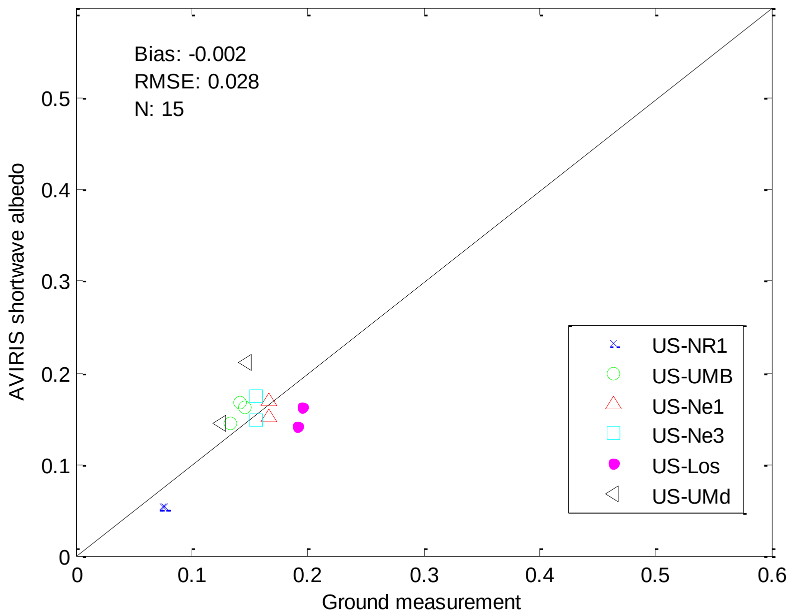

(a)

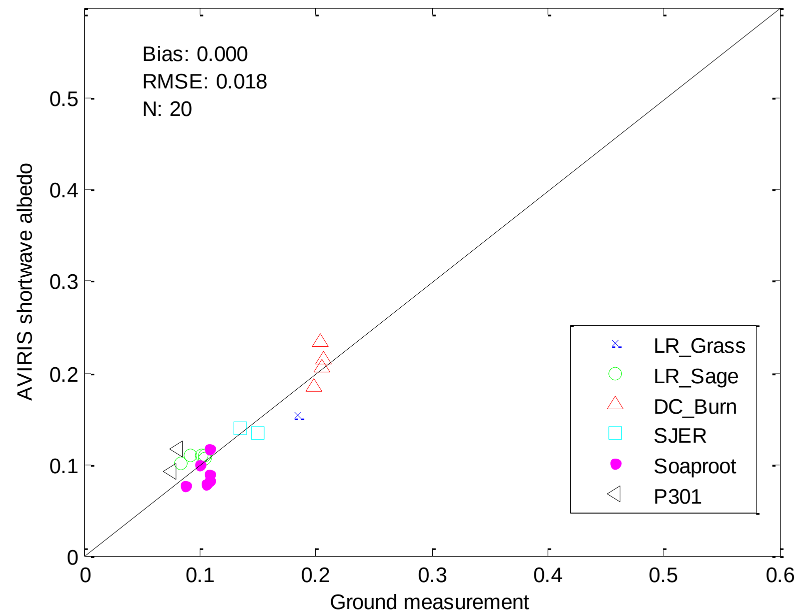

(b)

Validation of surface shortwave albedos at sites from (a) AmeriFlux network and (b) UCI network

Mapping surface albedo: AVIRIS vs. Landsat

(a)

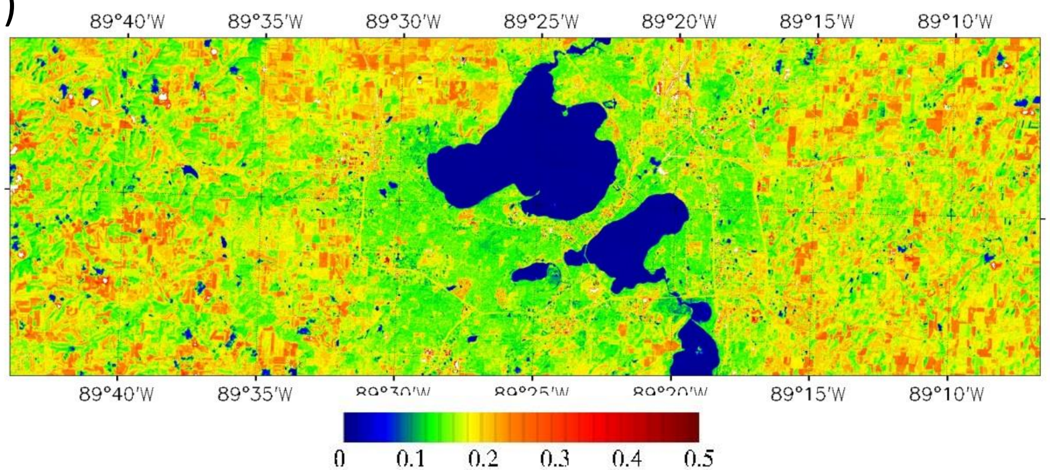

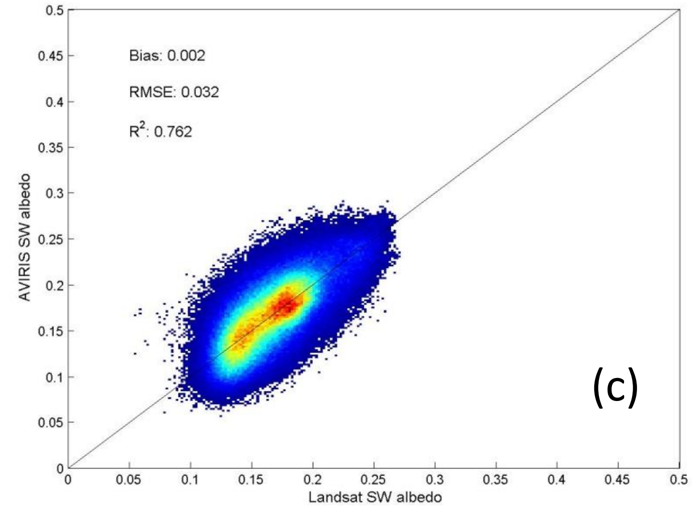

(b)

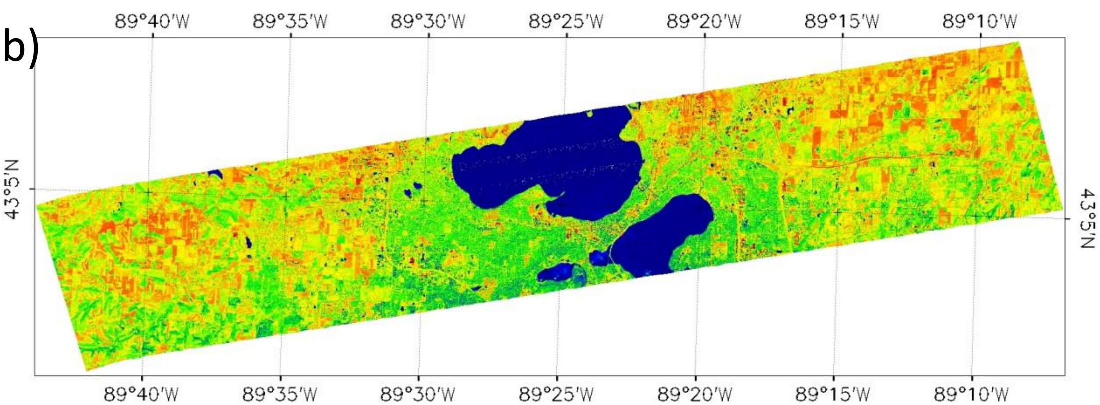

Shortwave albedo estimations from: (a) Landsat TM on Aug 18th, 2010; (b) AVIRIS on Aug 26th, 2010 using the stepwise regression algorithm; and (c) scatter plot. Image is centered at 43.08°N, 89.41°W in Madison, WI, USA.

Thank you!